

This discussion paper is/has been under review for the journal Atmospheric Chemistry and Physics (ACP). Please refer to the corresponding final paper in ACP if available.

**Examining the impact
of heterogeneous
nitryl chloride
production**

G. Sarwar et al.

Examining the impact of heterogeneous nitryl chloride production on air quality across the United States

G. Sarwar¹, H. Simon², P. Bhave¹, and G. Yarwood³

¹National Exposure Research Laboratory, US Environmental Protection Agency, Research Triangle Park, North Carolina, USA

²Office of Air Quality Planning and Standards, US Environmental Protection Agency, Research Triangle Park, North Carolina, USA

³ENVIRON International Corporation, Novato, California, USA

Received: 13 January 2012 – Accepted: 9 February 2012 – Published: 27 February 2012

Correspondence to: G. Sarwar (sarwar.golam@epamail.epa.gov)

Published by Copernicus Publications on behalf of the European Geosciences Union.

Title Page

Abstract

Introduction

Conclusions

References

Tables

Figures

⏪

⏩

◀

▶

Back

Close

Full Screen / Esc

Printer-friendly Version

Interactive Discussion

Abstract

The heterogeneous hydrolysis of dinitrogen pentoxide (N_2O_5) has typically been modeled as only producing nitric acid. However, recent field studies have confirmed that the presence of particulate chloride alters the reaction product to produce nitryl chloride (ClNO_2) which undergoes photolysis to generate chlorine atoms and nitrogen dioxide (NO_2). Both chlorine and NO_2 affect atmospheric chemistry and air quality. We present an updated gas-phase chlorine mechanism that can be combined with the Carbon Bond 05 mechanism and incorporate the combined mechanism into the Community Multiscale Air Quality modeling system. We then update the current model treatment of heterogeneous hydrolysis of N_2O_5 to include ClNO_2 as a product. The model, in combination with a comprehensive inventory of chlorine compounds, reactive nitrogen, particulate matter, and organic compounds, is used to evaluate the impact of the heterogeneous ClNO_2 production on air quality across the United States for the months of February and September in 2006. The heterogeneous production increases ClNO_2 in coastal as well as many in-land areas in the United States. Particulate chloride derived from sea-salts, anthropogenic sources, and forest fires activates the heterogeneous production of ClNO_2 . With current estimates of tropospheric emissions burden, it modestly enhances monthly mean 8-h ozone (up to 1–2 ppbv or 3–4 %) but causes large increases (up to 13 ppbv) in isolated episodes. It also substantially reduce the mean total nitrate by up to 0.8–2.0 $\mu\text{g m}^{-3}$ or 11–21 %. Modeled ClNO_2 accounts for up to 3–4 % of the monthly mean total reactive nitrogen. Sensitivity results of the model suggest that ClNO_2 formation is limited more by the presence of particulate chloride than by the abundance of N_2O_5 .

1 Introduction

Recent studies suggest that chlorine chemistry affects air quality in coastal and industrial areas of the United States (Chang et al., 2002; Knipping and Dabdub, 2003;

ACPD

12, 6145–6183, 2012

Examining the impact of heterogeneous nitryl chloride production

G. Sarwar et al.

Title Page

Abstract

Introduction

Conclusions

References

Tables

Figures

⏪

⏩

◀

▶

Back

Close

Full Screen / Esc

Printer-friendly Version

Interactive Discussion



Tanaka et al., 2003a; Chang and Allen, 2006; Sarwar and Bhawe, 2007; Simon et al., 2009). These studies have evaluated the effects of naturally- and anthropogenically-derived chlorine on ozone (O_3). First, Knipping and Dabdub (2003) reported that chlorine released via heterogeneous reactions on sea-salt particles increases daily maximum 1-h O_3 by up to 4 parts-per-billion (ppbv) in the Los Angeles area of California. Chang et al. (2002) and Chang and Allen (2006) concluded that industrial chlorine emissions increases O_3 by up to 10–16 ppbv in the Houston area of Texas. Finally, Sarwar and Bhawe (2007) found that anthropogenic chlorine emissions increase daily maximum 8-h O_3 by up to 4 ppbv in New York/New Jersey and 8 ppbv in the Houston areas.

In the past few years a new chlorine-containing species, nitryl chloride ($ClNO_2$), has been implicated as a major pathway for the production of reactive chlorine. Photolysis of $ClNO_2$ generates chlorine atoms (Cl) and nitrogen dioxide (NO_2); each can alter atmospheric chemistry and air quality. Finlayson-Pitts et al. (1989) first suggested that $ClNO_2$ could be an intermediate between aqueous-phase chloride and gas-phase chlorine radicals, but measurement technology did not exist to confirm this hypothesis in the ambient atmosphere. In the 2006 TexAQS-II field study, Osthoff et al. (2008) measured atmospheric $ClNO_2$ for the first time. They reported a peak value of greater than 1.0 ppbv near Houston. Results of several other recent field campaigns also suggested the presence of relatively high levels of $ClNO_2$ in coastal as well as in-land areas (Thornton et al., 2010; Mielke et al., 2010, 2011). These studies suggest that the main formation pathway for $ClNO_2$ is heterogeneous hydrolysis of dinitrogen pentoxide (N_2O_5) in the presence of particulate chloride. Simon et al. (2009) investigated the impact of measured $ClNO_2$ concentrations on O_3 in Houston using the Comprehensive Air quality Model with extensions (CAMx) and reported that it can enhance O_3 by up to 1.5 ppbv. While the Simon et al. (2009) study suggests $ClNO_2$ can modestly affect O_3 in Houston, little is known about the importance of $ClNO_2$ in other areas and seasons. In the current study, we examine the impacts of the heterogeneous $ClNO_2$ production on air quality in the United States using state-of-the-science knowledge about chlorine

Examining the impact of heterogeneous nitryl chloride production

G. Sarwar et al.

[Title Page](#)[Abstract](#)[Introduction](#)[Conclusions](#)[References](#)[Tables](#)[Figures](#)[⏪](#)[⏩](#)[◀](#)[▶](#)[Back](#)[Close](#)[Full Screen / Esc](#)[Printer-friendly Version](#)[Interactive Discussion](#)

chemistry and a detailed inventory of chlorine emissions.

2 Methodology

2.1 Model framework

This study uses the Community Multiscale Air Quality (CMAQ) modeling system (version 5.0; beta version) (Binkowski and Roselle, 2003; Byun and Schere, 2006; Foley et al., 2010) to simulate air quality. Evaluations for the CMAQ modeling system against ambient measurements have shown that CMAQ has considerable skill in simulating O₃ and fine particles (PM_{2.5}) (Eder and Yu, 2006; Appel et al., 2007; Foley et al., 2010). The modeling domain covers the entire United States and consists of 299 × 459 horizontal grid-cells with a 12-km resolution (see Fig. 1). The model contains 34 vertical layers with a surface layer height of 36-m. Model simulations were performed for February and September in 2006. Boundary conditions were generated from the GEOS-CHEM model (Bey et al., 2001) results. CMAQ results from a previous model simulation are used as initial conditions for this work. To further minimize the impact of initial conditions on predicted results, the model simulation started five days prior to the actual simulation periods. Meteorological fields were obtained from the Weather Research and Forecasting (version 3.3) model (Skamarock et al., 2008).

2.2 Emissions

The 2005 National Emissions Inventory (http://www.epa.gov/ttn/chief/net/2005_nei_point.pdf) is used to generate model-ready emissions using the Sparse Matrix Operator Kernel Emission (SMOKE) (Houyoux et al., 2000). The Biogenic Emissions Inventory System (version 3.14) is used to compute biogenic emissions from soil and vegetation (Schwede et al., 2005). Emissions of molecular chlorine (Cl₂) and hydrochloric acid (HCl) are included in the 2005 National Emissions Inventory. In addition, the fine-particulate emissions are speciated into the standard suite of compounds and trace

Examining the impact of heterogeneous nitryl chloride production

G. Sarwar et al.

Title Page

Abstract

Introduction

Conclusions

References

Tables

Figures



Back

Close

Full Screen / Esc

Printer-friendly Version

Interactive Discussion



elements (Reff et al., 2009). The largest sources of anthropogenic particulate chloride include paved and unpaved road dust, agricultural soil, wildfires, agricultural burning, coal/wood combustion, and diesel exhaust (Reff et al., 2009). Coarse particulate matter is also speciated to include particulate chloride. Road salt, one potentially important source of particulate chloride, is missing in the inventory. Fine and coarse sea-salt emissions (both open-ocean and surf-zone) are calculated in-line in CMAQ (Kelly et al., 2010).

2.3 Gas-phase chlorine chemistry

This study expands the CB05TU chemical mechanism (Whitten et al., 2010) to include additional chlorine chemistry. CB05TU builds on earlier work by Gery et al. (1989) and Yarwood et al. (2005) and includes 172 reactions involving 60 chemical species. These chemical mechanisms have been previously evaluated in the CMAQ model (Sarwar et al., 2008; Sarwar et al., 2011). Tanaka et al. (2003b) developed a chlorine mechanism consisting of 13 chemical reactions for use with an earlier version of this chemical mechanism. Here, we modify, and extend the chlorine mechanism of Tanaka et al. (2003b) for use with the CB05TU mechanism. Atmospheric reactions in the updated chlorine mechanism are shown in Table 1 (Reactions Cl1–Cl25). Rate constants for these reactions were updated using the recommendations from the International Union of Pure and Applied Chemistry (IUPAC) (Atkinson et al., 2005).

The new chlorine mechanism updates the chemistry developed by Tanaka et al. (2003b) in several ways. First, the chemistry is adjusted to new chemical species in the CB05TU mechanism. For example, the earlier mechanism grouped all aldehydes into a single lumped species, but the CB05TU mechanism splits acetaldehyde out from higher aldehydes. Similarly, the older mechanism included one olefin species, while the current mechanism separates compounds with internal carbon-carbon double bonds from those with a terminal carbon-carbon double bond (alk-1-enes). The new chlorine chemistry has been adjusted to account for these and other new species definitions. The reactions of formaldehyde, acetaldehyde, and higher aldehydes with

Examining the impact of heterogeneous nitril chloride production

G. Sarwar et al.

Title Page

Abstract

Introduction

Conclusions

References

Tables

Figures

⏪

⏩

◀

▶

Back

Close

Full Screen / Esc

Printer-friendly Version

Interactive Discussion



Cl are similar to their reactions with OH. The only exception is that the reaction with Cl produces HCl compared to H₂O produced from reactions with OH. The products of the reaction between higher aldehydes and Cl are uncertain because there may be hydrogen atom abstraction at the paraffinic carbon atoms of higher aldehydes.

5 Reaction products for terminal olefins with chlorine assume that reaction with the carbon-carbon double bond proceeds by addition, leading to cleavage of the double bond producing an acyl chloride (represented by formyl chloride) and an aldehyde (represented as 33 % acetaldehyde and 67 % higher aldehydes). The rate constant for the reaction between Cl and terminal olefins, Reaction (Cl14) is an average over
10 the absolute rate constants for the alkenes presented in Tanaka et al. (2003b). The rate constant for the reaction of chlorine with internal olefins, Reaction (Cl15) is estimated as the rate constant for Cl reacting with a terminal olefin bond and two paraffin bonds. The products assume that reaction proceeds 70 % by Cl addition to the C = C bond and 30 % by hydrogen atom abstraction from attached alkyl groups. Cl addition
15 leads to cleavage of the double bond producing an acyl chloride (represented by formyl chloride) and an aldehyde (represented as 65 % acetaldehyde and 35 % higher aldehydes). The products for hydrogen atom abstraction pathway are assumed to be HCl, higher aldehydes, and terminal olefins.

20 Second, the new chlorine chemistry includes more reactions of chlorine radicals with organic species including methanol, ethanol, aromatics, aldehydes, and ethane. The reaction between ethane and OH proceeds via the abstraction pathway and produces (in the presence of oxygen) ethyl peroxy radical and H₂O. The reaction of ethyl peroxy radical with NO can proceed via two different pathways. In one pathway, it converts NO into NO₂ and leads to acetaldehyde and HO₂ (99.1 %). In the other pathway, the
25 reaction leads to nitrate formation (0.9 %). The reaction of ethane with Cl also proceeds via the hydrogen abstraction pathway. With the exception of HCl rather than H₂O, its reaction products are same as the products of the reaction between ethane and OH, Reaction (Cl11). In addition, the products from the existing reaction with chlorine and isoprene were modified to more explicitly track the fate of Cl and carbon from isoprene.

Examining the impact of heterogeneous nitryl chloride production

G. Sarwar et al.

[Title Page](#)[Abstract](#)[Introduction](#)[Conclusions](#)[References](#)[Tables](#)[Figures](#)[Back](#)[Close](#)[Full Screen / Esc](#)[Printer-friendly Version](#)[Interactive Discussion](#)

The HCl and formyl chloride yields reflect the balance between hydrogen atom abstraction and addition pathways of 15% and 85% (Fan and Zhang; 2004). Formyl chloride serves as a surrogate for all products where chlorine is incorporated into a chlorocarbonyl after an addition reaction. Reaction of terpenes with Cl atoms is not included because the reaction products are too uncertain. Omitting the reaction may not greatly alter the fate of Cl atoms because Cl atoms react rapidly with all VOCs. For example, the global background for CH₄ of about 1.8 ppm (Oum et al., 1998) provides a significant “universal” sink for Cl atoms because Cl atoms react quite rapidly with CH₄.

The next major update to the Tanaka et al. (2003b) work is the inclusion of new reactions that lead to the formation of chlorine radicals including OH oxidation of HCl, Reaction (Cl4) and photolysis and oxidation of formyl chloride (Reactions Cl18 and Cl17). The new chemistry also includes both the gas-phase formation of ClNO₂, Reaction (Cl9) and its subsequent photolysis, Reaction (Cl3) as described by (Atkinson et al., 2005). In total, the updated chlorine mechanism contains five sources of reactive gas-phase Cl: photolysis of Cl₂, HOCl, ClNO₂, and reaction of HCl with OH, and the self-reaction of ClO, Reaction (Cl1–Cl5).

Normalized photolysis rates were used by Tanaka et al. (2003b). In the updated chlorine chemistry, photolysis rates, J , (min⁻¹) are directly calculated using the following general equation (Finlayson-Pitts and Pitts, 2000):

$$J = \int_{\lambda_1}^{\lambda_2} \sigma(\lambda)\phi(\lambda)F(\lambda)d\lambda \quad (1)$$

where, $\sigma(\lambda)$ is the absorption cross section (cm² molecule⁻¹), $\phi(\lambda)$ is the quantum yield (molecules photon⁻¹), $F(\lambda)$ is the actinic flux (photons cm² min⁻¹), λ is the wavelength (nm). Quantum yield and absorption cross-section data from the recent IUPAC recommendations are used in the mechanism (Atkinson et al., 2005). Photolysis of ClNO₂ can produce Cl and NO₂ in the presence of sunlight via Reaction (Cl3).

Examining the impact of heterogeneous nitryl chloride production

G. Sarwar et al.

Title Page

Abstract

Introduction

Conclusions

References

Tables

Figures

⏪

⏩

◀

▶

Back

Close

Full Screen / Esc

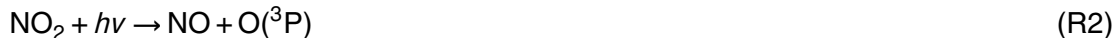
Printer-friendly Version

Interactive Discussion



Finally, rate constants for several reactions described by Tanaka et al. (2003b), have been updated to meet the latest recommendations of IUPAC (Atkinson et al., 2005): the reaction of Cl with O₃, Reaction (Cl5); the reaction of ClO with NO and HO₂ (Reactions Cl7–Cl8); the reaction of ethane and Cl (Reaction Cl13).

Chlorine chemistry affects O₃ primarily via two competing pathways that consume and produce O₃. It directly consumes O₃ via Reaction (Cl5). It also affects O₃ via reactions initiated by Cl and VOCs. Chlorine chemistry can enhance the oxidation of VOCs which then produce additional peroxy radicals (HO₂ and RO₂). The reaction of NO with HO₂ and RO₂ converts NO into NO₂ and cause O₃ production when NO₂ is photolyzed (Finlayson-Pitts and Pitts, 2000):



If additional O₃ production via Reactions (R1) and (R5) exceeds O₃ consumption via Reaction (Cl5), O₃ will increase.

2.4 Heterogeneous reaction

Although ClNO₂ can be formed in the gas phase through Reaction (Cl9), the high nighttime ClNO₂ concentrations observed in recent field campaigns are predominantly formed from reactions of N₂O₅ on particle surfaces. Current versions of CMAQ treat this heterogeneous N₂O₅ chemistry as producing only nitric acid, Reaction (R6).



Examining the impact of heterogeneous nitryl chloride production

G. Sarwar et al.

Title Page

Abstract

Introduction

Conclusions

References

Tables

Figures

⏪

⏩

◀

▶

Back

Close

Full Screen / Esc

Printer-friendly Version

Interactive Discussion

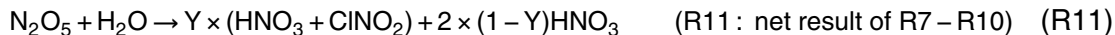


CMAQv5.0 calculates the rate constant of Reaction (R6) ($k_{\text{N}_2\text{O}_5,\text{het}}$) on fine PM using Eq. (2).

$$k_{\text{N}_2\text{O}_5,\text{het}} = \left(\frac{\tilde{d}}{2D} + \frac{4}{\bar{c}\gamma} \right)^{-1} A \quad (2)$$

In Eq. (2), d represents the effective diameter, D represents the diffusivity of N_2O_5 in air (as a function of temperature and pressure), \bar{c} is the mean molecular velocity of N_2O_5 (a function of temperature), A is the aerosol surface area concentration, and γ is the reactive uptake coefficient defined as the probability that a collision between an N_2O_5 molecule colliding with an aerosol particle will result in a reaction. The derivation of this equation is discussed in more detail elsewhere (Jacob, 2000). The CMAQ model calculates $\gamma_{\text{N}_2\text{O}_5}$ as a complex function of temperature, relative humidity, particle composition, and phase state (Davis et al., 2010).

The recent studies of Bertram and Thornton (2009) and Roberts et al. (2009) show that when particles contain chloride, ClNO_2 is also formed as a product via Reactions (R7–R10).



The yield of ClNO_2 (Y) represents the likelihood of $\text{NO}_2^+(\text{aq})$ reacting via Reaction (R9) versus Reaction (R10). This yield depends on the molar concentration of $\text{Cl}^-(\text{aq})$

Examining the impact of heterogeneous nitryl chloride production

G. Sarwar et al.

Title Page

Abstract

Introduction

Conclusions

References

Tables

Figures



Back

Close

Full Screen / Esc

Printer-friendly Version

Interactive Discussion



present in the particle and has been parameterized by Bertram and Thornton (2009) and Roberts et al. (2009). Both suggested a similar correlation (Eq. 3):

$$Y = \frac{1}{1 + \frac{k_9[\text{H}_2\text{O}(l)]}{k_{10}[\text{Cl}^-]}} \quad (3)$$

where $\text{H}_2\text{O}(l)$ = particle liquid water and Cl^- = particulate chloride. Bertram and Thornton (2009) derived a value of 483 for k_{10}/k_9 while Roberts et al. (2009) derived a value of 485 for k_{10}/k_9 . The formation of ClNO_2 in place of HNO_3 has implications for the reactive nitrogen budget since HNO_3 deposits quickly while ClNO_2 does not. Consequently, an increase in Y leads to increased availability of NO_x which participates in photochemical O_3 production outlined in Reactions (R1–R5).

Bertram and Thornton (2009) also suggested that the presence of particulate chloride can alter $\gamma_{\text{N}_2\text{O}_5}$ and developed a correlation (Eq. 4).

$$\gamma_{\text{N}_2\text{O}_5} = Ak'_{7f} \left(1 - \frac{1}{\left(\frac{k_9[\text{H}_2\text{O}(l)]}{k_{7b}[\text{NO}_3^-]} \right) + 1 + \left(\frac{k_{10}[\text{Cl}^-]}{k_{7b}[\text{NO}_3^-]} \right)} \right) \quad (4)$$

where $\text{H}_2\text{O}(l)$ = particle liquid water, NO_3^- = particulate nitrate, Cl^- = particulate chloride, $k_9/k_{7b} = 6 \times 10^{-2}$, $k_{10}/k_{7b} = 29$, $A = 3.2 \times 10^{-8}$, and k'_{7f} is calculated as follows:

$$k'_{7f} = \beta - \beta e^{-\delta[\text{H}_2\text{O}(l)]} \quad (5)$$

where, $\beta = 1.15 \times 10^{-6}$, and $\delta = 1.3 \times 10^{-1}$ (Bertram and Thornton, 2009).

In this study, we replace R6 with R11 in CMAQ. The yield and reactions rates are calculated separately for coarse and fine particles and use the chloride and water contents in the appropriately-size particles. The yield for Reaction (R11) is calculated with Eq. (3) on both fine and coarse particles. Reactive uptake ($\gamma_{\text{N}_2\text{O}_5}$) is calculated based

Examining the impact of heterogeneous nitryl chloride production

G. Sarwar et al.

Title Page

Abstract

Introduction

Conclusions

References

Tables

Figures

⏪

⏩

◀

▶

Back

Close

Full Screen / Esc

Printer-friendly Version

Interactive Discussion



Discussion Paper | Discussion Paper | Discussion Paper | Discussion Paper | Discussion Paper

on Davis et al. (2010) for fine particles (as is done in the base version of CMAQ) and is calculated based on Eq. (4) (using k_9/k_{10} from Bertram and Thornton, 2009) for coarse particles. To conserve mass of chlorine, particulate chloride mass is reduced by the amount of chlorine in ClNO_2 formed via the heterogeneous reaction on fine as well as coarse particles. If no particulate chloride is present, then $Y = 0$ according to Eq. (3) and no ClNO_2 is formed.

2.5 Simulation details

To evaluate the impacts of heterogeneous ClNO_2 formation on air quality, two different simulations were completed. The base simulation was conducted with $Y = 0$. Thus, only gas-phase reactions produced ClNO_2 . The other simulation was conducted with yield calculated from Eq. (3) so that the heterogeneous hydrolysis of N_2O_5 produces HNO_3 and ClNO_2 . Both the gas-phase and heterogeneous reactions produced ClNO_2 . Differences in the results obtained with the two simulations are attributed to the heterogeneous production of ClNO_2 .

3 Results and discussion

3.1 Model performance without heterogeneous ClNO_2 production

Model performance statistics for the base simulation without the heterogeneous ClNO_2 production for 8-h O_3 and daily mean $\text{PM}_{2.5}$ are shown in Tables 2 and 3. Ambient monitoring data from the United States Environmental Protection Agency's Air Quality System (AQS) are used to evaluate 8-h O_3 . We show statistics both for all 8-h max O_3 concentrations and for observed values above 65 ppbv to show how the model performs during high pollution episodes. The model captures observed 8-h O_3 data reasonably well. Model mean values are slightly greater than the observed values both in February and September. Ambient monitoring data from the AQS are used to

Examining the impact of heterogeneous nityl chloride production

G. Sarwar et al.

Title Page

Abstract

Introduction

Conclusions

References

Tables

Figures

⏪

⏩

◀

▶

Back

Close

Full Screen / Esc

Printer-friendly Version

Interactive Discussion



evaluate daily mean PM_{2.5} levels measured by the Federal Referenced Method (FRM). In addition, daily mean PM_{2.5} levels from the Interagency Monitoring of PROtected Visual Environments (IMPROVE) network and the Chemical Speciation Network (CSN) are also used to evaluate the model results. The model captures observed PM_{2.5} levels at all monitoring networks both in February and September. Model performance statistics are similar to or better than those for the previous versions of the model (Eder and Yu, 2006; Appel et al., 2007; Foley et al., 2010).

Predicted mean fine-particulate chloride levels in the base simulation are shown in Fig. 1a–b. Fine particulate chloride concentrations are highest in coastal areas and the Midwest. In addition, fine particulate chloride is present in the entire eastern half of the United States in February and Idaho in September. The fine particulate chloride in the eastern United States is largely derived from anthropogenic sources (mostly fugitive dust), while fine particulate chloride in the coastal areas comes mostly from sea salt. The high modeled levels in Idaho in September are due to particulate chloride emissions from a large wildfire. While the magnitudes of predicted levels are greater in September, predicted particulate chloride in February is present over a larger geographical area. Predicted mean coarse particulate chloride levels without the heterogeneous ClNO₂ production are shown in Fig. 1c–d.

Predicted fine particulate chloride levels averaged across all measurement sites in the United States are compared to the observed data from IMPROVE in Fig. 1e–f. With the exception of a few days in early February, average predictions are in good agreement with average observed data. Previous studies using the Tanaka et al. (2003b) chlorine chemistry and no ClNO₂ formation also showed reasonable performance of particulate chloride predictions. Kelly et al. (2010) compared CMAQ predictions to size resolved (both fine and coarse particles) particulate chloride observations from three coastal monitoring sites in Florida and reported good agreement between the model predictions and the observed data. Bhave and Appel (2009) compared CMAQ predictions to size resolved (both fine and coarse particles) particulate chloride observations from multiple monitoring sites in the United States and also reported good agreement.

Examining the impact of heterogeneous nitryl chloride production

G. Sarwar et al.

Title Page

Abstract

Introduction

Conclusions

References

Tables

Figures



Back

Close

Full Screen / Esc

Printer-friendly Version

Interactive Discussion



These results suggest model predicted fine and coarse particulate chloride levels are in good agreement with observed data and can be used to examine the impact of heterogeneous ClNO_2 production on air quality.

3.2 Impact of heterogeneous ClNO_2 chemistry on model performance statistics

The heterogeneous production of ClNO_2 marginally affects model performance statistics for daily maximum 8-h O_3 . For example, it changed the NMB from -20.2% to -18.8% in February and 0.1% to 0.4% in September for observed values above 65 ppbv . These changes which are mapped in Fig. S1 show that improvements and degradations in model performances do not have a noticeable geographic pattern. The inclusion of heterogeneous ClNO_2 formation also changed NME both in February and September by similar margins.

Predicted total nitrate (TNO_3) is compared with observed data from the Clean Air Status and Trends Network (CASTNet). Predicted TNO_3 without the heterogeneous production is greater than the observed data with NMB of 61.1% in February and 89.5% in September. Previous studies also reported over-predictions of nitrate (Foley et al., 2010). The over-predictions may be partially due to the $\gamma_{\text{N}_2\text{O}_5}$ parameterization used in the model. Brown et al. (2006) measured $\gamma_{\text{N}_2\text{O}_5}$ values in the eastern United States and reported the values to be much lower than those derived from model based approaches. All current $\gamma_{\text{N}_2\text{O}_5}$ parameterizations available in the peer-reviewed literature produce higher $\gamma_{\text{N}_2\text{O}_5}$ values. The heterogeneous production of ClNO_2 reduced the NMB to 57.1% in February and 85.9% in September for TNO_3 in the CASTNet. The heterogeneous production of ClNO_2 reduced the NMB from 64.2% to 61.2% in February and 42.1% to 36.4% in September for aerosol nitrate in the IMPROVE network. It also reduced the NMB from 44.8% to 41.7% in February and 67.7% to 60.5% in September for aerosol nitrate in the CSN. These improvements are shown in figures S2, S3, S4, and S5 and are most pronounced in the Eastern US in February where observed total nitrate concentrations are highest.

Examining the impact of heterogeneous nitryl chloride production

G. Sarwar et al.

Title Page

Abstract

Introduction

Conclusions

References

Tables

Figures



Back

Close

Full Screen / Esc

Printer-friendly Version

Interactive Discussion



Examining the impact of heterogeneous nitryl chloride production

G. Sarwar et al.

Title Page

Abstract

Introduction

Conclusions

References

Tables

Figures

⏪

⏩

◀

▶

Back

Close

Full Screen / Esc

Printer-friendly Version

Interactive Discussion

To evaluate the sensitivity of the model results to particulate chloride concentrations, two additional simulations were conducted with increased chlorine emissions [$3.0 \times$ (anthropogenic particulate chloride, Cl_2 , HCl) emissions used for the previous two simulations] for 10 days in February. One simulation was conducted without the heterogeneous production of ClNO_2 and the other simulation was conducted with the heterogeneous production of ClNO_2 . The additional chlorine emissions further increased ClNO_2 and O_3 and further decreased TNO_3 . Heterogeneous ClNO_2 chemistry combined with the augmented chlorine emissions increased mean ClNO_2 by up to 0.43 ppb compared to the value of 0.3 ppbv with the normal emissions. Similarly, heterogeneous ClNO_2 chemistry combined with the augmented emissions increased mean O_3 by up to 2.1 ppb compared to the value of 1.2 ppbv with the normal emissions. Mean O_3 in the northeast United States increased by 1.0–2.0 ppb with the augmented chlorine emissions, while mean O_3 increased by only 0.6–1.0 ppbv with the base case emissions. In the Midwest, this decrease in mean TNO_3 was 0.4–0.6 $\mu\text{g m}^{-3}$ compared to a value of 0.1–0.3 $\mu\text{g m}^{-3}$ with normal emissions. With the high chlorine emissions, heterogeneous ClNO_2 chemistry decreased mean TNO_3 in the Midwest by 0.4–0.6 $\mu\text{g m}^{-3}$ compared to the values of 0.1–0.3 $\mu\text{g m}^{-3}$ with the normal emissions. The impacts of heterogeneous ClNO_2 chemistry on ClNO_2 , O_3 and TNO_3 were more pronounced with the enhanced emissions. These results suggest that ClNO_2 formation is limited more by the presence of particulate chloride than by the abundance of N_2O_5 .

3.3 Predicted Y , ClNO_2 levels, and comparison with observed ClNO_2

Predicted mean values of Y on fine and coarse particles with the heterogeneous ClNO_2 production are presented in Fig. 2. As might be expected from Eq. (3), calculated yield is largest in areas in which particulate chloride concentrations are highest. Modeled yields on fine particles reached values above 0.7 in many coastal and in-land areas. Yield values on coarse particles reached 1.0 over the Gulf and the Oceans and ranged between 0.1 and 0.8 in coastal and in-land areas. These modeled yields suggest that

the presence of particulate chloride can efficiently activate the heterogeneous ClNO_2 production pathway throughout large areas of the United States.

Modeled mean ClNO_2 levels in the base simulation that included only the gas-phase formation pathway (no heterogeneous ClNO_2 production) are negligible (generally < 0.5 pptv) and are not discussed further. Heterogeneous production enhanced ClNO_2 levels both in February and September. Predicted monthly mean and the hourly maximum ClNO_2 levels during the entire month with the heterogeneous production are presented in Fig. 3. ClNO_2 formed where particulate chloride and NO_x concentrations are prevalent. The highest monthly mean predicted ClNO_2 was found in the Los Angeles area both in February (0.3 ppbv) and in September (0.5 ppbv). Mean ClNO_2 concentrations also reached moderate values of around 0.1 to 0.2 ppbv in portions of the Northeast during both September and February. While predicted values reached higher concentrations in September, predicted levels are more spatially distributed in February. The maximum hourly predicted value in February reached almost 3.0 ppbv in Los Angeles and 2.0 ppbv in the Midwest. High hourly ClNO_2 concentrations in September were found in Idaho (4.5 ppbv maximum) and in Los Angeles (4.0 ppbv maximum). Predicted ClNO_2 levels were consistently high in Los Angeles both in February and September. Available chlorine to produce ClNO_2 in coastal areas comes from sea-salt emissions and in the Midwest comes from anthropogenic chloride emissions. In addition, chlorine available to enhance ClNO_2 over the eastern half of the United States in February is due to anthropogenic emissions and over Idaho is due to chlorine emissions from the forest fires in September.

Ambient ClNO_2 levels are not routinely measured; these measurements are conducted only in specialized field campaigns. To our knowledge, four sets of measurements have been published in the peer-reviewed literature. A qualitative comparison of predicted ClNO_2 levels with these measurements is presented in Table 4. Osthoff et al. (2008) measured ClNO_2 in Houston in 2006 and reported a peak value of about 1200 pptv. Predicted peak ClNO_2 in Houston reached 2000 pptv in February and 1500 pptv in September. Thornton et al. (2010) reported a peak value of

Examining the impact of heterogeneous nitryl chloride production

G. Sarwar et al.

Title Page

Abstract

Introduction

Conclusions

References

Tables

Figures



Back

Close

Full Screen / Esc

Printer-friendly Version

Interactive Discussion

450 pptv in Boulder, Colorado in February 2009. The predicted peak value in Boulder was 300 pptv in February and 200 pptv in September. Mielke et al. (2011) reported a peak ClNO_2 value of 250 pptv in Calgary, Canada in April 2010. The predicted peak value in Calgary reached 500 pptv in February and 300 pptv in September. Mielke et al. (2010) reported a peak value of 2,550 pptv in Los Angeles, California in June 2010. The predicted peak value in Los Angeles reached 2700 pptv in February and 4000 pptv in September. Predicted levels are similar to the observed values reported in the literature. Based on these comparisons, the model parameterizations of yield and $\gamma_{\text{N}_2\text{O}_5}$ along with our emissions of NO_x and gas and particle-phase chlorine compounds appear to do a reasonable job of replicating the chemistry that leads to ClNO_2 production.

3.4 Impact of the heterogeneous ClNO_2 production on selected gaseous and particle species

3.4.1 Monthly mean concentrations

Monthly mean O_3 levels in the base simulation and changes due to the heterogeneous production are presented in Fig. 4. Monthly mean O_3 levels between 30 and 50 ppbv in February and between 40 and 65 ppbv in September were modeled over most areas in the United States. The heterogeneous ClNO_2 production enhanced monthly mean O_3 by a maximum of 1.3 ppbv in February and 1.4 ppbv in September. On a percentage basis, the enhancement reached up to 4% and 3% in February and September, respectively. Enhancements in February occurred over a larger geographic area than those in September. Predictions of ClNO_2 occurred over a wider area in February; consequently ozone enhancements also occurred over a larger geographic area. Although not shown here, the heterogeneous ClNO_2 production enhanced mean HO_2 and RO_2 by a few percent. These radicals increased primarily due to the oxidation of VOCs by Cl which is produced via the photolysis of ClNO_2 . Enhancements of O_3 in the heterogeneous ClNO_2 formation simulation were due both to the increased HO_2 and

Examining the impact of heterogeneous nitryl chloride production

G. Sarwar et al.

Title Page

Abstract

Introduction

Conclusions

References

Tables

Figures

⏪

⏩

◀

▶

Back

Close

Full Screen / Esc

Printer-friendly Version

Interactive Discussion



RO₂ radicals and due to the increased availability of NO₂.

Monthly mean total nitrate (TNO₃) levels in the base simulation and changes due to the heterogeneous production are presented in Fig. 5. Here we define TNO₃ as the sum of gas-phase HNO₃ and fine and coarse particle nitrate. Mean TNO₃ levels of more than 4.0 μg m⁻³ are predicted over most of the eastern United States and southern California in February and over parts of Midwest, southern United States, and southern California in September. The activation of the heterogeneous ClNO₂ pathway reduced the production of HNO₃ via the N₂O₅ hydrolysis which then decreased TNO₃ both in February and September. The mean decreases in February were up to 0.8 μg m⁻³ while the decrease in September reached 2.0 μg m⁻³. On a percentage basis, the reductions were up to 11 % and 21 % in February and September, respectively. Both high nitrate concentrations and large nitrate decreases covered a broader area in February than in September.

The heterogeneous ClNO₂ production also enhanced sulfate by <0.1 μg m⁻³, decreased ammonium by <0.3 μg m⁻³, and increased anthropogenic and biogenic secondary organic aerosols by <0.003 μg m⁻³. These changes are due to shifts in the radical budget and NO_x availability and are not discussed further in this paper.

3.4.2 Day-to-day variation

Several areas were identified as having high modeled ClNO₂ concentrations in Sect. 3.3. Here we examine the temporally-resolved changes in ClNO₂, O₃, and TNO₃ in those areas. Time series of the changes in ClNO₂, O₃, and TNO₃ due to the heterogeneous production in Los Angeles, Indiana, and Idaho are shown Fig. 6. These values are averaged over each representative region and since ClNO₂ formation chemistry can occur in localized areas, this analysis does not show the maximum impact of that chemistry. Figure 6 shows that ClNO₂ concentrations increase every night in Los Angeles in both February and September. Predicted increases in ClNO₂ in February are lower than those in September in Los Angeles. Nightly concentrations averaged

Examining the impact of heterogeneous nitryl chloride production

G. Sarwar et al.

Title Page

Abstract

Introduction

Conclusions

References

Tables

Figures

⏪

⏩

◀

▶

Back

Close

Full Screen / Esc

Printer-friendly Version

Interactive Discussion



over the Los Angeles area range 0.15 ppbv to above 1.0 ppbv. These fairly routine ClNO₂ episodes are due to the constant source of particulate chloride from sea-salt and NO_x from mobile sources. Ozone enhancements and TNO₃ decrease due to the ClNO₂ chemistry are predicted daily in Los Angeles and range from 0.3 to 3 ppb for O₃ and from 0.1 to 4.0 μg m⁻³ for TNO₃. Anthropogenic particulate chloride emissions are responsible for the chlorine available for heterogeneous production in Indiana and enhanced ClNO₂ and O₃, and decreased TNO₃ on most days in February. Chloride and NO_x emissions from a large wildfire in Idaho activated the heterogeneous production and increased ClNO₂ and O₃ up to 1 ppbv and 2.5 ppbv respectively and decreased TNO₃ by up to 2.5 μg m⁻³ over a large portion of Idaho. The wildfire was active only during the first part in September and consequently the heterogeneous production during the second part in September is negligible. Thus, the heterogeneous ClNO₂ production is active on most days in some areas while it is activated by sporadic events such as wildfires or large industrial emissions in other areas.

3.4.3 Diurnal variation of the impact

Figure 7 shows average diurnal changes in ClNO₂, O₃, and TNO₃ in Los Angeles, Indiana, and the northeastern United States due to the heterogeneous production of ClNO₂. Again, these changes are averaged over each representative area. ClNO₂ increased during the course of the night, reached peak levels in the early morning and then decreased due to the photolysis and dropped to its lowest level in the afternoon. The peak ClNO₂ levels in February occurred somewhat later in the morning than those in September due to the lower photolysis rate and late sun rise. The modeled diurnal pattern of ClNO₂ agrees well with observed profile reported by Thornton et al. (2010). The O₃ enhancement started in the morning and reached a peak value in the afternoon and then decreased. The time of peak O₃ increase varied by season; O₃ enhancements reached their peak around noon September and later in the afternoon in February. So even though ClNO₂ photolysis released Cl radicals and NO₂ in

Examining the impact of heterogeneous nitryl chloride production

G. Sarwar et al.

Title Page

Abstract

Introduction

Conclusions

References

Tables

Figures

⏪

⏩

◀

▶

Back

Close

Full Screen / Esc

Printer-friendly Version

Interactive Discussion

the first several hours after sunrise, these model simulations predict that its effect on O_3 continues well into the day meaning that $ClNO_2$ production will have a noticeable impact of 8-h daily maximum O_3 , the regulatory metric used to identify areas in violation with national air quality standards in the US. The decrease in TNO_3 followed the same diurnal pattern as the changes in $ClNO_2$ since the decrease of HNO_3 is a direct result of the heterogeneous N_2O_5 chemistry following the pathway of $ClNO_2$ formation Reaction (R10) rather than HNO_3 production Reaction (R9). Similar diurnal pattern of the changes in $ClNO_2$, O_3 , TNO_3 were observed in other areas.

3.4.4 Impact on daily maximum 8-h O_3

Predicted mean 8-h O_3 in the base simulation and enhancements due to the heterogeneous production are presented in Fig. 8. Predicted mean 8-h O_3 without the heterogeneous production are greater than 46 ppbv in most of the United States in September while predicted values are lower than 46 ppbv in February. The heterogeneous production enhanced the monthly mean 8-h O_3 by up to 1.7 ppbv in February and 1.9 ppbv in September. On a percentage basis, the enhancement reached up to 4% and 3% in February and September, respectively. The largest monthly mean impact occurred in Los Angeles both in February and September. The largest enhancement in daily maximum 8-h O_3 in any grid-cell was 13.3 ppbv in February and 6.6 ppbv in September. On a percentage basis, the largest enhancement in daily maximum 8-h O_3 in any grid-cell was 43% in February and 10% in September. Although mean enhancements in maximum 8-h O_3 are modest, impacts on specific days can be quite large.

3.5 Impact on the composition of total reactive nitrogen (NO_y)

The mean $ClNO_2:NO_y$ ratios without the heterogeneous $ClNO_2$ production are negligible (< 0.001). Heterogeneous $ClNO_2$ production increased mean $ClNO_2:NO_y$ ratios up to 0.04 in February and 0.03 in September. As TNO_3 concentrations decreased with heterogeneous $ClNO_2$ production, so did their contribution to NO_y . While the

Examining the impact of heterogeneous nitryl chloride production

G. Sarwar et al.

Title Page

Abstract

Introduction

Conclusions

References

Tables

Figures

⏪

⏩

◀

▶

Back

Close

Full Screen / Esc

Printer-friendly Version

Interactive Discussion



mean $\text{ClNO}_2:\text{NO}_Y$ ratios were small, the maximum hourly $\text{ClNO}_2:\text{NO}_Y$ ratios are much greater and reached 0.34 in February and 0.17 in September. The contribution of ClNO_2 to NO_Y was generally greater in February than in September; thus, the ratio was also higher in February.

5 3.6 Impact of $\gamma_{\text{N}_2\text{O}_5}$ parameterization on model predictions

The presence of particulate chloride can increase $\gamma_{\text{N}_2\text{O}_5}$ value as described by Bertram and Thornton (2009). However particulate chloride is not explicitly accounted for in the $\gamma_{\text{N}_2\text{O}_5}$ which is described by Davis et al. (2010) and used in the current version of CMAQ. The Davis et al. (2010) parameterization was also used to calculate the heterogeneous reaction rate on fine particles in this work. To evaluate the sensitivity of the model results to $\gamma_{\text{N}_2\text{O}_5}$, two additional simulations were completed for a 10-day period in each month. The first simulation employed $\gamma_{\text{N}_2\text{O}_5}$ (Eq. 4) of Bertram and Thornton (2009) on both fine and coarse particles and used $Y = 0$. The second simulation employed $\gamma_{\text{N}_2\text{O}_5}$ of Bertram and Thornton (2009) on both fine and coarse particles with Y calculated using Eq. (3). The differences in results obtained with the two simulations are compared to those obtained with the previous two simulations employing $\gamma_{\text{N}_2\text{O}_5}$ of Davis et al. (2010) on fine particles and $\gamma_{\text{N}_2\text{O}_5}$ of Bertram and Thornton (2009) on coarse particles. While enhancements in hourly O_3 obtained with the two $\gamma_{\text{N}_2\text{O}_5}$ varied occasionally by 1-2 ppbv, the enhancements in mean 8-h O_3 obtained with the two $\gamma_{\text{N}_2\text{O}_5}$ did not differ significantly (<0.2 ppb). The decreases in hourly as well as mean TNO_3 obtained with $\gamma_{\text{N}_2\text{O}_5}$ of Bertram and Thornton (2009) on both fine and coarse particles were greater than those obtained with the modeling simulations described in the main portion of this paper. The additional mean decreases ranged up to $0.4\text{--}1.4 \mu\text{g m}^{-3}$. Thus, the use of $\gamma_{\text{N}_2\text{O}_5}$ of Bertram and Thornton (2009) on both fine and coarse particles can further reduce TNO_3 without further enhancement of O_3 .

Examining the impact of heterogeneous nitryl chloride production

G. Sarwar et al.

Title Page

Abstract

Introduction

Conclusions

References

Tables

Figures

⏪

⏩

◀

▶

Back

Close

Full Screen / Esc

Printer-friendly Version

Interactive Discussion



4 Summary

Heterogeneous ClNO₂ chemistry is successfully implemented into the CMAQ model along with a comprehensive inventory of chlorine and reactive nitrogen emissions. While the homogeneous production of ClNO₂ is negligible, the heterogeneous production enhances ClNO₂ in coastal areas, the eastern half of the United States, and Idaho. Sea-salt derived particulate chloride enhances ClNO₂ in coastal areas while anthropogenic particulate chloride enhances ClNO₂ in the eastern half of the United States and chloride from forest fires enhances ClNO₂ in Idaho. Mean ClNO₂ levels increase by up to 0.3 ppbv in February and 0.5 ppbv in September though the maximum hourly values are much greater.

Predicted ClNO₂ enhances monthly mean 8-h O₃ modestly. It can, however, decrease mean TNO₃ by larger margins and improve model performance statistics. Predicted ClNO₂ reaches its peak level in the early morning while the O₃ enhancement starts in the morning and reaches a peak value in the afternoon. The impact of the heterogeneous production occurs over a larger geographical area in February. The heterogeneous production of ClNO₂ changes the composition of NO_γ; predicted ClNO₂ can account for up to 3–4 % of the monthly mean NO_γ but up to 34 % of NO_γ in some localized episodes.

The results of this study compare favorably to the findings of Simon et al. (2009) who reported that the heterogeneous ClNO₂ production can increase daily maximum 8-h O₃ in Houston by up to 1.5 ppbv. While the heterogeneous ClNO₂ production in this study enhances monthly mean 8-h O₃ by less than 0.2 ppbv in Houston, it enhanced the daily maximum 8-h O₃ by levels similar to those reported by Simon et al. (2009). It should be noted that Simon et al. (2009) used 4-km grid resolution and this study uses 12-km grid resolution. Since the modeling domain covers the entire United States, a larger grid resolution is used in this study. Emissions of NO_x and VOCs used by Simon et al. (2009) are also different than those used in this study. One large improvement over the modeling formulation presented in that work is that this modeling uses generalized

Examining the impact of heterogeneous nitryl chloride production

G. Sarwar et al.

Title Page

Abstract

Introduction

Conclusions

References

Tables

Figures



Back

Close

Full Screen / Esc

Printer-friendly Version

Interactive Discussion

parameterizations for reactive uptake and ClNO_2 yield while Simon et al. (2009) relied on local measurements to create fixed values for those variables. Our new model formulation has allowed for the investigation of the effects ClNO_2 chemistry over the entire continental United States and over multiple seasons. Our predicted yields in Houston are lower than the fixed 0.75 value used by Simon et al. (2009). Results of this study suggest that the effect of ClNO_2 production on air quality is more pronounced in several areas in the United States than it is in Houston. Field campaigns in those areas could validate the findings in this study.

Supplementary material related to this article is available online at:

<http://www.atmos-chem-phys-discuss.net/12/6145/2012/acpd-12-6145-2012-supplement.pdf>.

Disclaimer. Although this paper has been reviewed by EPA and approved for publication, it does not necessarily reflect EPA's policies or views.

References

- Appel, K. W., Gilliland, A. B., Sarwar, G., and Gilliam, R. C.: Evaluation of the Community Multiscale Air Quality (CMAQ) model version 4.5: Sensitivities impacting model performance, Part I-Ozone, Atmos. Environ., 41, 9603–9615, 2007.
- Atkinson, R., Baulch, D. L., Cox, R. A., Crowley, J. N., Hampson, R. F., Hynes, R. G., Jenkin, M. E., Kerr, J. A., Rossi, M. J., and Troe, J.: Summary of evaluated kinetic and photochemical data for atmospheric chemistry – IUPAC subcommittee on gas kinetic data evaluation for atmospheric chemistry, available at: <http://www.iupac-kinetic.ch.cam.ac.uk/index.html>, 2005.
- Bhave, P. V. and Appel, K. W.: Evaluation of the CMAQ Model for Size-Resolved PM Composition, 8th Annual CMAS Models-3 Users' Conference, 19–21 October, available at: <http://www.cmascenter.org/conference/2009/agenda.cfm>, UNC-Chapel Hill, NC, 2009.
- Bertram, T. H. and Thornton, J. A.: Toward a general parameterization of N_2O_5 reactivity on aqueous particles: the competing effects of particle liquid water, nitrate and chloride, Atmos. Chem. Phys., 9, 8351–8363, doi:10.5194/acp-9-8351-2009, 2009.

Examining the impact of heterogeneous nitryl chloride production

G. Sarwar et al.

Title Page

Abstract

Introduction

Conclusions

References

Tables

Figures



Back

Close

Full Screen / Esc

Printer-friendly Version

Interactive Discussion



**Examining the impact
of heterogeneous
nitryl chloride
production**G. Sarwar et al.

[Title Page](#)[Abstract](#)[Introduction](#)[Conclusions](#)[References](#)[Tables](#)[Figures](#)[⏪](#)[⏩](#)[◀](#)[▶](#)[Back](#)[Close](#)[Full Screen / Esc](#)[Printer-friendly Version](#)[Interactive Discussion](#)

- Bey, I., Jacob, D. J., Yantosca, R. M., Logan, J. A., Field, B. D., Fiore, A. M., Li, Q., Liu, H. Y., Mickley, L. J., and Schultz, M. G.: Global modeling of tropospheric chemistry with assimilated meteorology: Model description and evaluation, *J. Geophys. Res.*, 106, 23073–23096, 2001.
- 5 Binkowski, F. S. and Roselle, S. J.: Community Multiscale Air Quality (CMAQ) model aerosol component, I: Model description, *J. Geophys. Res.*, 108, 4183, doi:10.1029/2001JD001409, 2003.
- Brown, S. S., Ryerson, T. B., Wollny, A. G., Brock, C. A., Peltier, R., Sullivan, A. P., Weber, R. J., Dube, W. P., Trainer, M., Meagher, J. F., Fehsenfeld, F. C., and Ravishankara, A. R.: Variability in nocturnal nitrogen oxide processing and its role in regional air quality, *Science*, 10 311, 67–70, 2006.
- Byun, D. and Schere, K. L.: Review of the governing equations, computational algorithms, and other components of the Models-3 Community Multiscale Air Quality (CMAQ) modeling system, *Appl. Mech. Rev.*, 59, 51–77, 2006.
- 15 Chang, S. and Allen, D. T.: Atmospheric chlorine chemistry in Southeast Texas: Impacts on ozone formation and control, *Environ. Sci. Technol.*, 40, 251–262, 2006.
- Chang, S., McDonald-Buller, E. C., Kimura, Y., Yarwood, G., Neece, J., Russel, M., Tanaka, P., and Allen, D.: Sensitivity of urban ozone formation to chlorine emission estimates, *Atmos. Environ.*, 36, 4991–5003, 2002.
- Davis, J. M., Bhawe, P. V., and Foley, K. M.: Parameterization of N_2O_5 reaction probabilities on the surface of particles containing ammonium, sulfate, and nitrate, *Atmos. Chem. Phys.*, 8, 20 5295–5311, doi:10.5194/acp-8-5295-2008, 2008.
- Eder, B. and Yu, S.: A performance evaluation of the 2004 release of Models-3 CMAQ, *Atmos. Environ.*, 40, 4811–4824, 2004.
- Fan, J. and Zhang, R.: Atmospheric Oxidation mechanism of isoprene, *Environ. Chem.*, 1, 25 140–149, 2004.
- Finlayson-Pitts, B. J., Ezell, J. J., and Pitts Jr., J. N.: Formation of chemically active chlorine compounds by reactions of atmospheric NaCl particles with gaseous N_2O_5 and $ClONO_2$, *Nature*, 337, 241–244, 1989.
- Finlayson-Pitts, B. J. and Pitts Jr., J. N.: *Chemistry of the Upper Lower Atmosphere, Theory, Experiments and Applications*, Academic Press, San Diego, 2000.
- 30 Foley, K. M., Roselle, S. J., Appel, K. W., Bhawe, P. V., Pleim, J. E., Otte, T. L., Mathur, R., Sarwar, G., Young, J. O., Gilliam, R. C., Nolte, C. G., Kelly, J. T., Gilliland, A. B., and Bash, J. O.: Incremental testing of the Community Multiscale Air Quality (CMAQ) modeling system

Examining the impact of heterogeneous nitril chloride production

G. Sarwar et al.

Title Page

Abstract

Introduction

Conclusions

References

Tables

Figures

⏪

⏩

◀

▶

Back

Close

Full Screen / Esc

Printer-friendly Version

Interactive Discussion

version 4.7, Geosci. Model Dev., 3, 205–226, doi:10.5194/gmd-3-205-2010, 2010.

Gery, M. W., Whitten, G. Z., Killus, J. P., and Dodge, M. C.: A photochemical kinetics mechanism for urban and regional scale computer modeling, *J. Geophys. Res.*, 94, 12925–12956, 1989.

5 Houyoux, M. R., Vukovich, J. M., Coats Jr., C. J., Wheeler, N. M., and Kasibhatla, P. S.: Emission inventory development and processing for the seasonal model for regional air quality (SMRAQ) project, *J. Geophys. Res.*, 105, 9079–9090, 2000.

Jacob, D. J.: Heterogeneous chemistry and tropospheric ozone, *Atmos. Environ.*, 34, 2131–2159, 2000.

10 Kelly, J. T., Bhawe, P. V., Nolte, C. G., Shankar, U., and Foley, K. M.: Simulating emission and chemical evolution of coarse sea-salt particles in the Community Multiscale Air Quality (CMAQ) model, *Geosci. Model Dev.*, 3, 257–273, doi:10.5194/gmd-3-257-2010, 2010.

Knipping, E. M. and Dabdub, D.: Impact of chlorine emissions from sea-salt aerosol on coastal urban ozone, *Environ. Sci. Technol.*, 37, 275–284, 2003.

15 Mielke, L. H., Flynn, J. H., Grossberg, N., Lefer, B. L., Veres, P. R., Roberts, J. M., Froyd, K. D., Cochran, A. K., and Osthoff, H. D.: Quantification and analysis of CalNex-LA 2010, American Geophysical Union, Fall Meeting 2010, San Francisco, California, available at: <http://adsabs.harvard.edu/abs/2010AGUFM.A21C0118M>, 2010.

Mielke, L. H., Furgeson, A., and Osthoff, H. D.: Observation of ClNO₂ in a mid-continent urban environment, *Environ. Sci. Technol.*, 45, 8889–8896, 2011.

20 Osthoff, H. D., Roberts J. M., Ravishankara, A. R., Williams, E. J., Lerner, B. M., Sommariva, R., Bates, T. S., Coffman D., Quinn P. K., Dibb, J. E., Stark H., Burkholder J. B., Talukdar, R. K., Meagher, J. M., Fehsenfeld, F. C., and Brown, S. S.: High levels of nitril chloride in the polluted subtropical marine boundary layer, *Nat. Geosci.*, 1, 324–328, 2008.

25 Oum, K. W., Lakin, M. J., DeHaan, D. O., Brauers, T., and Finlayson-Pitts, B. J.: Formation of molecular chlorine from the photolysis of ozone and aqueous sea-salt particles, *Science*, 279, 74–77, 1998.

Reff, A., Bhawe, P. V., Simon, H., Pace, T. G., Pouliot, G. A., Mobley, J. D., and Houyoux, M.: Emissions inventory of PM_{2.5} trace elements across the United States, *Environ. Sci. Technol.*, 43, 5790–5796, 2009.

30 Roberts, J. M., Osthoff, H. D., Brown, S. S., Ravishankara, A. R., Coffman, D., Quinn, P., and Bates, T.: Laboratory studies of products of N₂O₅ uptake on Cl⁻ containing substrates, *Geophys. Res. Lett.*, 36, L20808, doi:10.1029/2009GL040448, 2009.

- Sarwar, G., Luecken, D., Yarwood, G., Whitten, G., and Carter, B.: Impact of an updated Carbon Bond mechanism on air quality using the Community Multiscale Air Quality modeling system: preliminary assessment, *J. Appl. Meteorol. Clim.*, 47, 3–14, 2008.
- Sarwar, G., Appel, K. W., Carlton, A. G., Mathur, R., Schere, K., Zhang, R., and Majeed, M. A.: Impact of a new condensed toluene mechanism on air quality model predictions in the US, *Geosci. Model Dev.*, 4, 183–193, doi:10.5194/gmd-4-183-2011, 2011.
- Sarwar, G. and Bhawe, P.: Modeling the effect of chlorine emissions on atmospheric ozone across the eastern United States, *J. Appl. Meteorol. Clim.*, 46, 1009–1019, 2007.
- Schwede, D., Pouliot, G., and Pierce, T.: Changes to the biogenic emissions inventory system version 3 (BEIS3), 4th Annual CMAS Models-3 Users' Conference, 26–28 September 2005, UNC-Chapel Hill, NC, available at: http://www.cmascenter.org/html/2005_conference/abstracts/2.7.pdf, 2005.
- Simon, H., Kimura, Y., McGaughey, G., Allen, D. T., Brown, S. S., Osthoff, H. D., Roberts, J. M., Byun, D., and Lee, D.: Modeling the impact of ClNO₂ on ozone formation in the Houston area, *J. Geophys. Res.*, 114, D00F03, doi:10.1029/2008JD010732, 2009.
- Smith, J. D., DeSain, J. D., and Taatjes, C. A.: Infrared laser absorption measurements of HCl(*v* = 1) production in reactions of Cl atoms with isobutane, methanol, acetaldehyde, and toluene at 295 K, *Chem. Phys. Lett.*, 366, 417–425, 2002.
- Tanaks, P. L., Riemer, D. D., Chang, S. H., Yarwood, G., McDonald-Buller, E. C., Apel, E. C., Orlando, J. J., Silva, P. F., Jimenez, J. L., Canagaratna, M. R., Neece, J. D., Mullins, C. B., and Allen, D. T.: Direct evidence for chlorine-enhanced urban ozone formation in Houston, Texas, *Atmos. Environ.*, 37, 1393–1400, 2003a.
- Tanaka, P., Allen, D. T., McDonald-Buller, E.C., Chang, S., Kimura, Y., Mullins, C. B., Yarwood, G., and Neece, J. D.: Development of a chlorine mechanism for use in the carbon bond IV chemistry model, *J. Geophys. Res.*, 108, 4145, 6–1:13, doi: 10.1029/2002JD002432, 2003b.
- Thornton, J. A., Kercher J. P., Riedel T. P., Wagner N. L., Cozic J., Holloway J. S., Dube W. P, Wolfe G. M., Quinn P. K., Middlebrook A. M., Alexander B., and Brown S. S.: A large atomic chlorine source inferred from mid-continental reactive nitrogen chemistry, *Nature*, 464, 271–274, 2010.
- Yarwood, G., Rao, S., Yocke, M., and Whitten, G.: Updates to the Carbon Bond Chemical Mechanism: CB05, Final Report to the US EPA, RT-0400675, available at: www.camx.com, 2005.

Examining the impact of heterogeneous nitryl chloride production

G. Sarwar et al.

[Title Page](#)[Abstract](#)[Introduction](#)[Conclusions](#)[References](#)[Tables](#)[Figures](#)[⏪](#)[⏩](#)[◀](#)[▶](#)[Back](#)[Close](#)[Full Screen / Esc](#)[Printer-friendly Version](#)[Interactive Discussion](#)

**Examining the impact
of heterogeneous
nitryl chloride
production**

G. Sarwar et al.

[Title Page](#)[Abstract](#)[Introduction](#)[Conclusions](#)[References](#)[Tables](#)[Figures](#)[⏪](#)[⏩](#)[◀](#)[▶](#)[Back](#)[Close](#)[Full Screen / Esc](#)[Printer-friendly Version](#)[Interactive Discussion](#)

- Yu, S., Dennis, R. L., Bhawe, P. V., and Eder, B. K.: Primary and secondary organic aerosols over the United States: estimates on the basis of observed organic carbon (OC) and elemental carbon (EC), and air quality modeled primary OC/EC ratios, *Atmos. Environ.*, **38**, 5257–5268, 2004.
- 5 Wallington, T. J., Skewes, L. M., and Siegl, W. O.: Kinetics of the gas phase reaction of chlorine atoms with a series of alkenes, alkynes and aromatic species at 295 K, *J. Photochem. Photobiol. A*, **45**, 167–175, 1988.
- Whitten, G. Z., Heo, G., Kimura, Y., McDonald-Buller, E., Allen, D., Carter, W. P. L., and Yarwood, G.: A new condensed toluene mechanism for Carbon Bond: CB05-TU, *Atmos. Environ.*, **44**, 5346–5355, 2010.
- 10

Table 1. Reactions in the chlorine mechanism for use with the CB05 mechanism.

No.	Reactants	Products	Rate Expression ^a	Ref
Cl1	Cl2	2 × Cl	Photolysis	b
Cl2	HOCl	OH + Cl	Photolysis	b
Cl3	ClNO ₂	Cl + NO ₂	Photolysis	b
Cl4	OH + HCl	Cl + H ₂ O	$6.58 \times 10^{-13} (T/300)^{1.16} e^{(-58/T)}$	c
Cl5	Cl + O ₃	ClO + O ₂	$2.3 \times 10^{-11} e^{(-200/T)}$	b
Cl6	ClO + ClO	0.3 × Cl ₂ + 1.4 × Cl + O ₂	1.63×10^{-14}	b
Cl7	ClO + NO	Cl + NO ₂	$6.4 \times 10^{-12} e^{(290/T)}$	b
Cl8	ClO + HO ₂	HOCl + O ₂	$2.7 \times 10^{-12} e^{(220/T)}$	b
Cl9	Cl + NO ₂	ClNO ₂	$k_o = 1.8 \times 10^{-31} (T/300)^{-2.0}$ $k_{\infty} = 1.0 \times 10^{-10} (T/300)^{-1.0}$ $F = 0.6$ and $N = 1.0$	b
Cl10	Cl + CH ₄	HCl + MEO ₂	$6.6 \times 10^{-12} e^{(-1240/T)}$	b
Cl11	Cl + ETHA	HCl + 0.991 × ALD ₂ + 0.991 × XO ₂ + 0.009 × XO ₂ N + HO ₂	$8.3 \times 10^{-11} e^{(-100/T)}$	b
Cl12	Cl + PAR	HCl + 0.87 × XO ₂ + 0.13 × XO ₂ N + 0.11 × HO ₂ + 0.06 × ALD ₂ − 0.11 × PAR + 0.76 × ROR + 0.05 × ALDX	5.00×10^{-11}	b
Cl13	Cl + ETH	FMCl + 2.0 × XO ₂ + HO ₂ + FORM	1.07×10^{-10}	b
Cl14	Cl + OLE	FMCl + 0.33 × ALD ₂ + 0.67 × ALDX + 2.0 × XO ₂ + HO ₂ -PAR	2.5×10^{-10}	b
Cl15	Cl + IOLE	0.3 × HCl + 0.7 × FMCl + 0.45 × ALD ₂ + 0.55 × ALDX + 0.3 × OLE + 0.3 × PAR + 1.7 × XO ₂ + HO ₂	3.5×10^{-10}	b
Cl16	Cl + ISOP	0.15 × HCl + XO ₂ + HO ₂ + 0.85 × FMCl + ISPD	4.3×10^{-10}	b,d
Cl17	OH + FMCl	Cl + CO + H ₂ O	5.0×10^{-13}	b
Cl18	FMCl	Cl + CO + HO ₂	Photolysis	b
Cl19	Cl + FORM	HCl + HO ₂ + CO	$8.2 \times 10^{-11} e^{(-34/T)}$	b
Cl20	Cl + ALD ₂	HCl + C ₂ O ₃	7.9×10^{-11}	b
Cl21	Cl + ALDX	HCl + CXO ₃	1.3×10^{-10}	b
Cl22	Cl + MEOH	HCl + HO ₂ + FORM	5.5×10^{-11}	b
Cl23	Cl + ETOH	HCl + HO ₂ + ALD ₂	$8.2 \times 10^{-11} e^{(45/T)}$	b
Cl24	Cl + TOL	HCl + 0.88 × XO ₂ + 0.88 × HO ₂ + 0.12 × XO ₂ N	6.1×10^{-11}	e
Cl25	Cl + XYL	HCl + 0.84 × XO ₂ + 0.84 × HO ₂ + 0.16 × XO ₂ N	1.2×10^{-10}	f

Note:

^a First order rate constants are in units of s^{-1} , second order rate constants are in units of $cm^3 \text{ molecule}^{-1} s^{-1}$. Temperatures (T) are in Kelvin. Rate constants for reaction 7 is described by the falloff expression of the form $k = \{k_o[M]/(1+k_o[M]/k_\infty)\} F^Z$, where $Z = \{(1/N) + \log_{10}[k_o [M]/k_\infty]^2\}^{-1}$, where $[M]$ is the total pressure in molecules cm^{-3} , and k_o , k_∞ , F , and N are indicated in table.

Ref: ^b = Atkinson et al., 2005; ^c = Keene et al., 2007; ^d = Fan and Zhang; 2004; ^e = Smith et al., 2002; ^f = Wallington et al., 1988.

Cl_2 = molecular chlorine, Cl = atomic chlorine, $HOCl$ = hypochlorous acid, $ClNO_2$ = nitryl chloride, HCl = hydrochloric acid, OH = hydroxyl radical, O_2 = oxygen, O_3 = ozone, ClO = chlorine oxide, NO = nitric oxide, NO_2 = nitrogen dioxide, H_2O = water vapor, HO_2 = hydroperoxy radical, $FMCl$ = formyl chloride, CO = carbon monoxide, CH_4 = methane, $ETHA$ = ethane, MEO_2 = methylperoxy radical, PAR = paraffin carbon bond, XO_2 = NO-to- NO_2 operator, XO_2N = NO-to-nitrate operator, $FORM$ = formaldehyde, ALD_2 = acetaldehyde, $ALDX$ = propionaldehyde and higher aldehydes, OLE = terminal olefinic carbon bond, IOL = internal olefinic carbon bond, ETH = ethene, $ISOP$ = isoprene, $ISPD$ = isoprene product, $MEOH$ = methanol, $ETOH$ = ethanol, C_2O_3 = acetylperoxy radical, CXO_3 = higher acylperoxy radicals, ROR = secondary organic oxy radical, TOL = toluene, XYL = xylene. The chlorine mechanism adds seven chemical species to CB05.

ACPD

12, 6145–6183, 2012

Examining the impact of heterogeneous nitryl chloride production

G. Sarwar et al.

Title Page

Abstract

Introduction

Conclusions

References

Tables

Figures

⏪

⏩

◀

▶

Back

Close

Full Screen / Esc

Printer-friendly Version

Interactive Discussion



Examining the impact of heterogeneous nitryl chloride production

G. Sarwar et al.

[Title Page](#)[Abstract](#)[Introduction](#)[Conclusions](#)[References](#)[Tables](#)[Figures](#)[⏪](#)[⏩](#)[◀](#)[▶](#)[Back](#)[Close](#)[Full Screen / Esc](#)[Printer-friendly Version](#)[Interactive Discussion](#)

Table 2. Model performance statistics for 8-h O₃.

Metric	AQS		AQS (obs > 65 ppbv)	
	February 8-h O ₃	September 8-h O ₃	February 8-h O ₃	September 8-h O ₃
Number of observations	14 873	20 019	22	912
Mean modeled (ppbv)	39.5	49.8	55.0	73.6
Mean observed (ppbv)	36.4	40.5	69.0	73.7
Median modeled (ppbv)	40.8	48.8	55.8	72.1
Median observed (ppbv)	37.1	39.2	68.3	70.8
NMB(%)	8.5	22.9	-20.2	-0.1
NME(%)	17.5	26.4	20.2	11.8
MB(ppb)	3.1	9.2	-14.0	-0.1
ME (ppb)	6.4	10.7	14.0	8.7

NMB = Normalized Mean Bias, NME = Normalized Mean Error, ME = Mean Error, MB = Mean Bias

Examining the impact of heterogeneous nitryl chloride production

G. Sarwar et al.

Table 3. Model performance statistics for daily mean PM_{2.5}.

Metric	AQS FRM Sites		IMPROVE		CSN	
	February Daily mean PM _{2.5}	September Daily mean PM _{2.5}	February Daily mean PM _{2.5}	September Daily mean PM _{2.5}	February Daily mean PM _{2.5}	September Daily mean PM _{2.5}
Number of observations	9553	5998	1348	831	949	628
Mean modeled ($\mu\text{g m}^{-3}$)	15.2	11.9	5.7	5.3	17.1	12.0
Mean observed ($\mu\text{g m}^{-3}$)	11.6	9.7	4.4	5.3	11.0	9.4
Median modeled ($\mu\text{g m}^{-3}$)	12.7	10.4	3.3	3.5	14.4	11.0
Median observed ($\mu\text{g m}^{-3}$)	9.8	8.3	2.9	4.0	11.0	8.8
NMB(%)	31.1	22.8	33.2	0.0	28.0	28.1
NME(%)	52.6	38.9	56.1	41.7	51.8	45.0
MB($\mu\text{g m}^{-3}$)	3.8	2.2	1.4	0.0	3.8	2.6
ME ($\mu\text{g m}^{-3}$)	6.1	3.8	2.4	2.2	6.9	4.2

FRM = Federal Reference Method

- Title Page
- Abstract Introduction
- Conclusions References
- Tables Figures
- Navigation (Left/Right arrows)
- Back Close
- Full Screen / Esc
- Printer-friendly Version
- Interactive Discussion



Examining the impact of heterogeneous nitryl chloride production

G. Sarwar et al.

Title Page

Abstract

Introduction

Conclusions

References

Tables

Figures

⏪

⏩

◀

▶

Back

Close

Full Screen / Esc

Printer-friendly Version

Interactive Discussion



Table 4. A comparison of predicted nitryl chloride with observed data.

Measurement location	Measurement time period	References	Peak measurement value (pptv)	Peak prediction in February (pptv)	Peak prediction in September (pptv)
Houston, Texas	8/30–9/8/2006	Osthoff et al. (2008)	1200	2000	1500
Boulder, Colorado	2/11–2/25/2009	Thornton et al. (2010)	450	300	200
Calgary, Alberta	4/16–4/21/2010	Mielke et al. (2011)	250	500	300
Los Angeles, California	5/15–6/15/2010	Mielke et al. (2010)	2550	2700	4000

Examining the impact of heterogeneous nitryl chloride production

G. Sarwar et al.

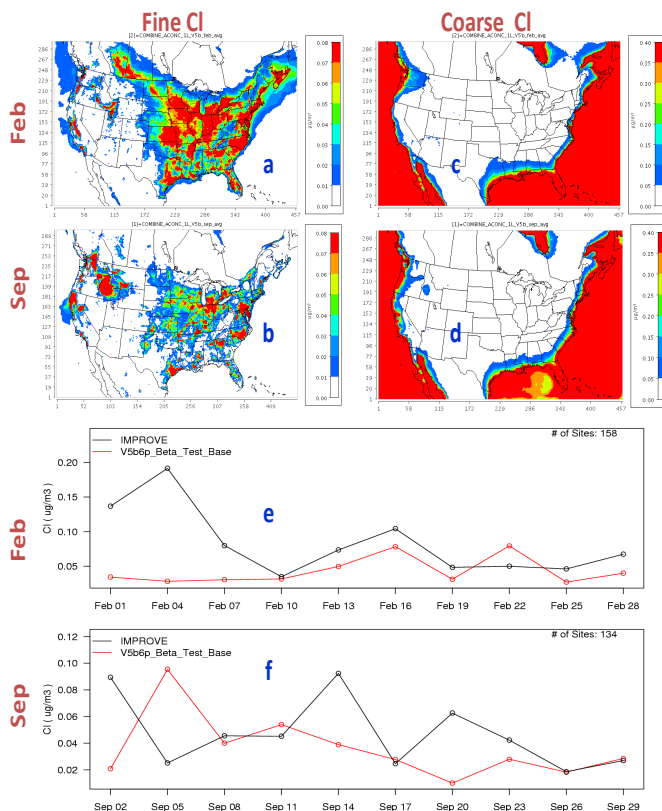


Fig. 1. Predicted mean fine particulate chloride without the heterogeneous ClNO_2 production in (a) February and (b) September. Predicted mean coarse particulate chloride without the heterogeneous ClNO_2 production in (c) February and (d) September. A comparison of predicted fine particulate chloride with observed data from the Interagency Monitoring of PROtected Visual Environments (IMPROVE) network in (e) February and (f) September.

Title Page

Abstract Introduction

Conclusions References

Tables Figures

◀ ▶

◀ ▶

Back Close

Full Screen / Esc

Printer-friendly Version

Interactive Discussion



Examining the impact of heterogeneous nitryl chloride production

G. Sarwar et al.

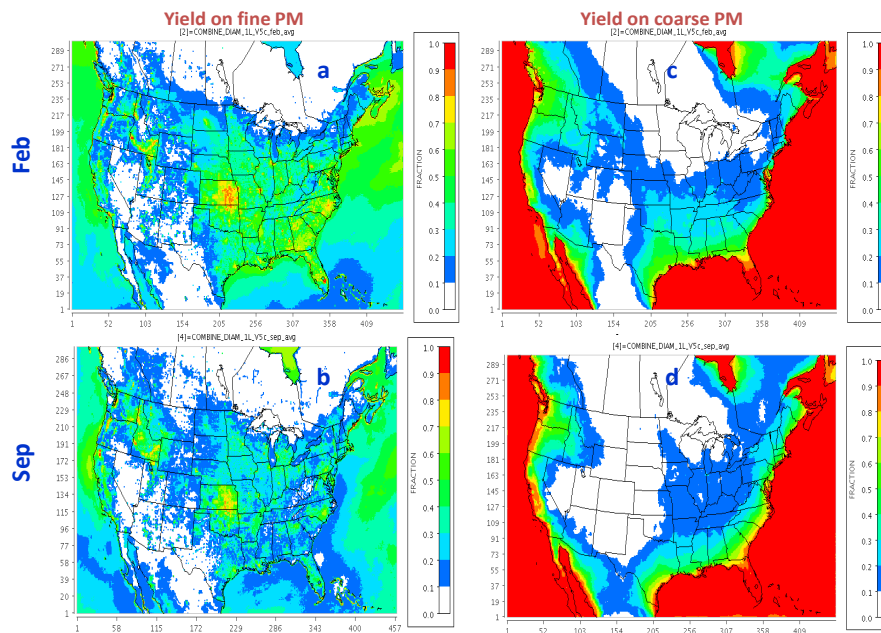


Fig. 2. (a) Predicted mean yield for $CINO_2$ on fine particles in (a) February and (b) September. Predicted mean yield for $CINO_2$ on coarse particles in (c) February and (d) September.

[Title Page](#)[Abstract](#)[Introduction](#)[Conclusions](#)[References](#)[Tables](#)[Figures](#)[⏪](#)[⏩](#)[◀](#)[▶](#)[Back](#)[Close](#)[Full Screen / Esc](#)[Printer-friendly Version](#)[Interactive Discussion](#)

Examining the impact of heterogeneous nitryl chloride production

G. Sarwar et al.

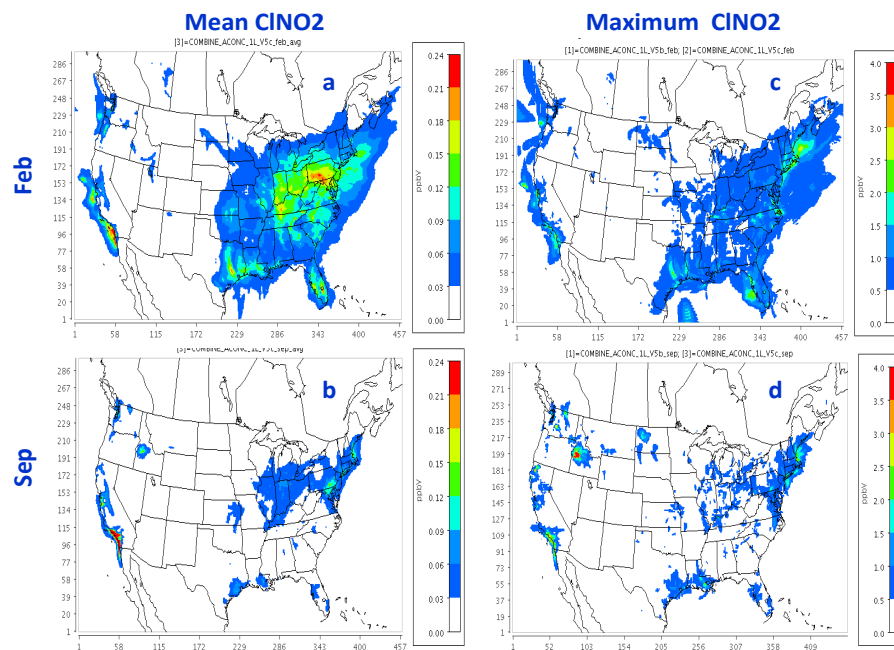


Fig. 3. Predicted mean CINO₂ in (a) February (b) September and maximum CINO₂ in (c) February (d) September. It should be noted that the largest hourly value for each grid-cell in the entire month is shown in (c) and (d).

Title Page

Abstract

Introduction

Conclusions

References

Tables

Figures

⏪

⏩

◀

▶

Back

Close

Full Screen / Esc

Printer-friendly Version

Interactive Discussion

Examining the impact of heterogeneous nitryl chloride production

G. Sarwar et al.

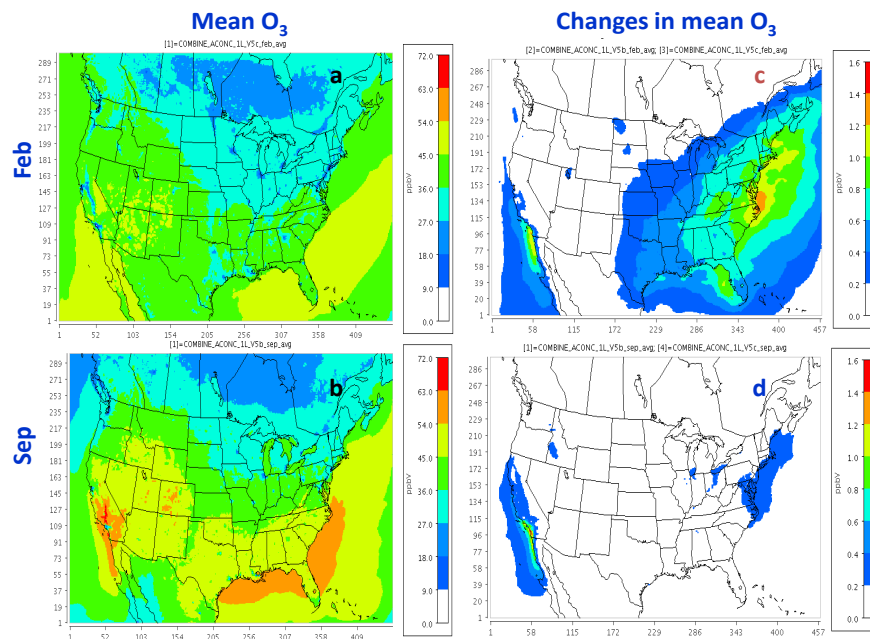


Fig. 4. Impact of the heterogeneous ClNO₂ production on O₃: **(a)** mean O₃ without the heterogeneous production in February **(b)** mean O₃ without the heterogeneous production in September **(c)** increases in mean O₃ due to the heterogeneous production in February **(d)** increases in mean O₃ due to the heterogeneous production in September.

[Title Page](#)[Abstract](#)[Introduction](#)[Conclusions](#)[References](#)[Tables](#)[Figures](#)[◀](#)[▶](#)[◀](#)[▶](#)[Back](#)[Close](#)[Full Screen / Esc](#)[Printer-friendly Version](#)[Interactive Discussion](#)

Examining the impact of heterogeneous nitryl chloride production

G. Sarwar et al.

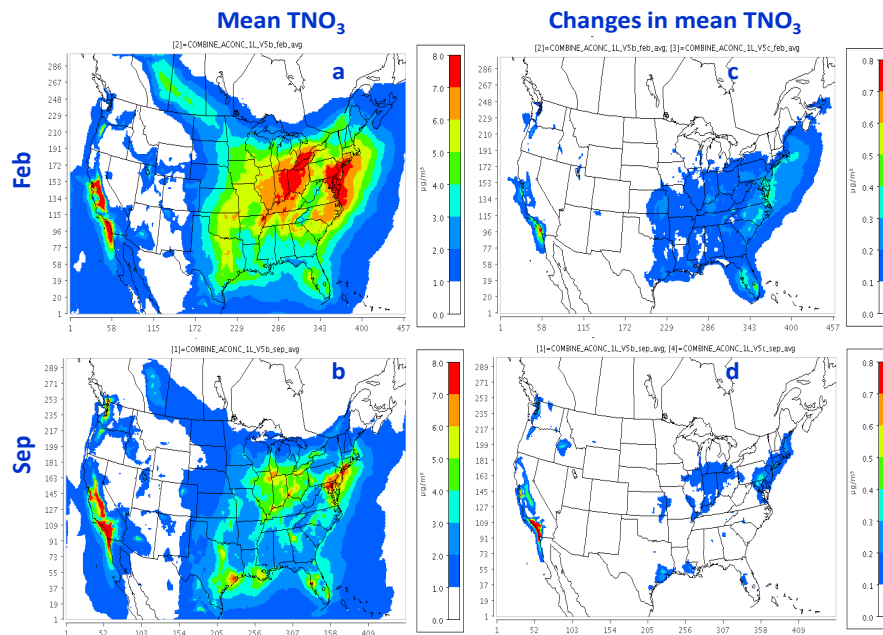


Fig. 5. Impact of the heterogeneous CINO₂ production on TNO₃ (HNO₃ + aerosol nitrate): **(a)** mean TNO₃ without the heterogeneous production in February **(b)** mean TNO₃ without the heterogeneous production in September **(c)** decreases in mean TNO₃ due to the heterogeneous production in February **(d)** decreases in mean TNO₃ due to the heterogeneous production in September.

Title Page

Abstract

Introduction

Conclusions

References

Tables

Figures

⏪

⏩

◀

▶

Back

Close

Full Screen / Esc

Printer-friendly Version

Interactive Discussion

Examining the impact of heterogeneous nitryl chloride production

G. Sarwar et al.

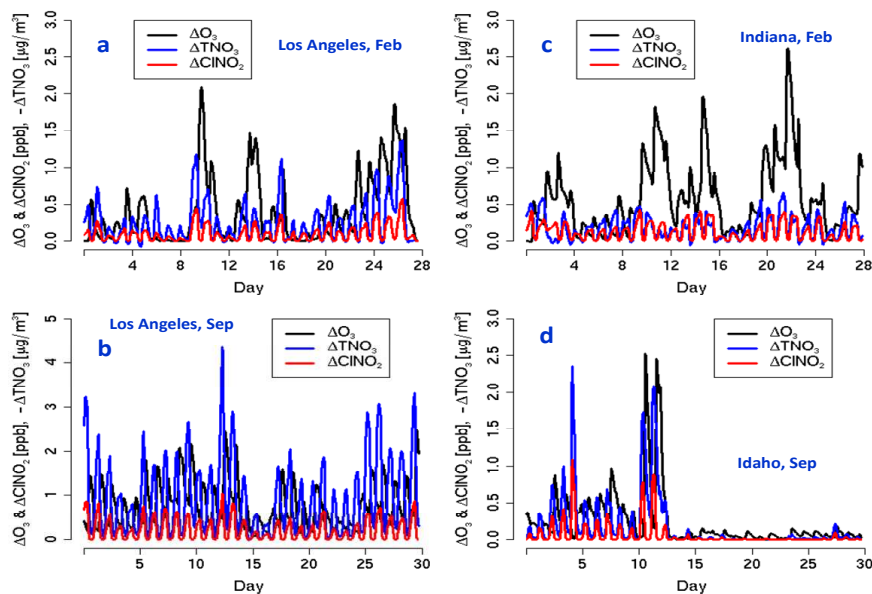


Fig. 6. Time series of the absolute value of changes in CINO₂, O₃, and -TNO₃ at (a) Los Angeles in February (b) Los Angeles in September (c) Indiana in February (d) Idaho in September. All Δ values are positive for O₃ and CINO₂ and negative for TNO₃.

Title Page

Abstract

Introduction

Conclusions

References

Tables

Figures

⏪

⏩

◀

▶

Back

Close

Full Screen / Esc

Printer-friendly Version

Interactive Discussion

Examining the impact of heterogeneous nitryl chloride production

G. Sarwar et al.

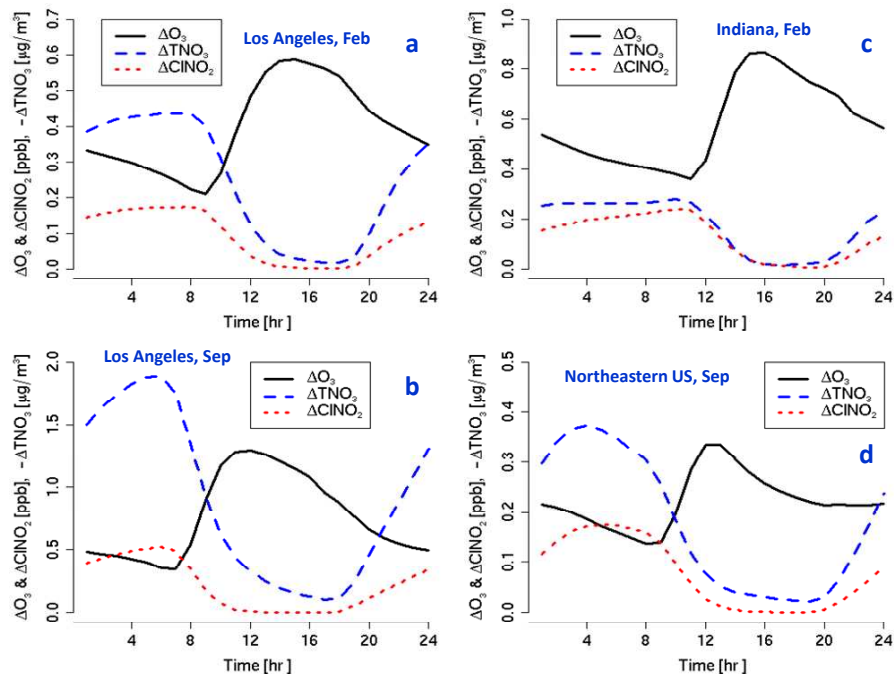


Fig. 7. Diurnal absolute value of changes in CINO_2 , O_3 , and $-\text{TNO}_3$ at (a) Los Angeles in February (b) Los Angeles in September (c) Indiana in February (d) Northeastern United States in September. All Δ values are positive for O_3 and CINO_2 and negative for TNO_3 .

Title Page

Abstract

Introduction

Conclusions

References

Tables

Figures

◀

▶

◀

▶

Back

Close

Full Screen / Esc

Printer-friendly Version

Interactive Discussion

Examining the impact of heterogeneous nitryl chloride production

G. Sarwar et al.

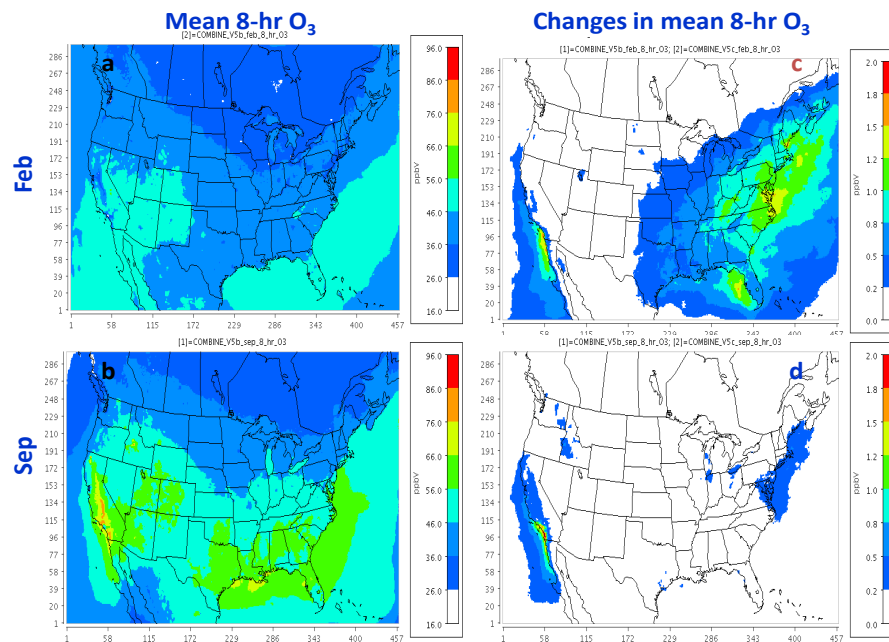


Fig. 8. (a) Predicted mean 8-h O₃ in February (b) Predicted mean 8-h O₃ in September (c) changes in mean 8-h O₃ due to the heterogeneous production in February (d) changes in mean 8-h O₃ due to the heterogeneous production in September.

[Title Page](#)[Abstract](#)[Introduction](#)[Conclusions](#)[References](#)[Tables](#)[Figures](#)[⏪](#)[⏩](#)[⏴](#)[⏵](#)[Back](#)[Close](#)[Full Screen / Esc](#)[Printer-friendly Version](#)[Interactive Discussion](#)